

Spatial coherence in complex photonic and plasmonic systems

A. Cazé, R. Pierrat and R. Carminati*

Institut Langevin, ESPCI ParisTech, CNRS, 1 rue Jussieu, 75238 Paris Cedex 05, France

The concept of cross density of states characterizes the intrinsic spatial coherence of complex photonic or plasmonic systems, independently on the illumination conditions. Using this tool and the associated intrinsic coherence length, we demonstrate unambiguously the spatial squeezing of eigenmodes on disordered fractal metallic films, thus clarifying a basic issue in plasmonics.

PACS numbers: 78.67.-n, 42.25.Dd, 73.20.Mf, 32.50.+d

The optical properties of nanostructured materials have attracted a lot of attention, due to their potential for light concentration and transport at subwavelength scales [1, 2]. New possibilities have emerged, for the design of efficient sources and absorbers of visible and near-infrared radiation, or for optical storage and information processing with ultrahigh spatial density. Metallic nanostructures benefit from the excitation of surface plasmons that permit concentration at ultra-small length scales and ultra-fast time scales [3]. Periodic materials structured at scales on the order of the wavelength (photonic crystals) [4] or below the wavelength (metamaterials) [5] benefit from bandgap effects or artificial effective properties going beyond that of natural materials. Disordered media also offer the possibility to build up spatially localized modes (e.g. by the process of Anderson localization) [6]. Light concentration and transport at sub-wavelength scales encompass a broad range of processes, including coherent control at the nanoscale [7], enhancement of light-matter interaction in weak and strong coupling regimes [8–12], superradiance [13], enhancement of non-radiative energy transfer [14], or light focusing beyond the diffraction limit [15–17]. The spatial extent of eigenmodes is of central importance, since it characterizes the ability of the system to support concentrated or delocalized excitations. It drives, e.g., the coherence length of surface plasmons [12, 18–21], the range of non-radiative energy transfer [22, 23], or the lower limit for spatial focusing by time reversal or phase conjugation [24–26]. The trade-off between localized and delocalized excitations is also a central issue for the understanding and the control of the optical properties of disordered fractal metallic films [27]. In this Letter, we introduce the Cross Density Of States (CDOS) as a quantity that characterizes the overall spatial extent of eigenmodes, and use it to address the spatial localization of light on disordered fractal metallic films. We demonstrate unambiguously the spatial squeezing of eigenmodes close to the percolation threshold, thus providing a theoretical basis to clarify a controversial issue in plasmonics [8, 28–30]. This also illustrates the relevance of the CDOS to characterize the intrinsic spatial coherence in photonics and plasmonics

systems.

In order to characterize the intrinsic spatial coherence of complex photonic or plasmonic system at a given frequency ω , we introduce a two-point quantity $\rho(\mathbf{r}, \mathbf{r}', \omega)$ that we will refer to as CDOS, defined as

$$\rho(\mathbf{r}, \mathbf{r}', \omega) = \frac{2\omega}{\pi c^2} \text{Im} [\text{Tr} \mathbf{G}(\mathbf{r}, \mathbf{r}', \omega)] . \quad (1)$$

In this expression, c is the speed of light in vacuum, $\mathbf{G}(\mathbf{r}, \mathbf{r}', \omega)$ is the electric dyadic Green function that connects the electric field at point \mathbf{r} to an electric-dipole source \mathbf{p} at point \mathbf{r}' through the relation $\mathbf{E}(\mathbf{r}) = \mu_0 \omega^2 \mathbf{G}(\mathbf{r}, \mathbf{r}', \omega) \mathbf{p}$, and Tr denotes the trace of a tensor.

The choice of this quantity as a measure of the intrinsic spatial coherence results from the observation that the imaginary part of the Green function at two different points appears in a number of situations where the spatial coherence of random fields (produced by random sources and/or a disordered medium) needs to be characterized [6, 31–33]. The imaginary part of the Green function also describes the process of focusing by time reversal in a closed cavity [24, 25]. The precise definition of the CDOS in Eq. (1) has been chosen so that it reduces to the Local Density Of States (LDOS) when \mathbf{r} and \mathbf{r}' coincide [2, 34].

The physical picture behind the CDOS is a counting of optical eigenmodes that connect two different points at a given frequency. In a network picture, the LDOS measures the number of channels crossing at a given point, whereas the CDOS measures the number of channels connecting two points. In order to give a more rigorous basis to this picture, let us consider the canonical situation of a non-absorbing system (e.g., a nanostructured material) placed in a closed cavity. In this case an orthonormal discrete basis of eigenmodes can be defined, with eigenfrequencies ω_n and eigenvectors $\mathbf{e}_n(\mathbf{r})$. The expansion of the dyadic Green function reads $\mathbf{G}(\mathbf{r}, \mathbf{r}', \omega) = \sum_n c^2 \mathbf{e}_n^*(\mathbf{r}') \mathbf{e}_n(\mathbf{r}) / (\omega_n^2 - \omega^2)$ where the superscript $*$ stands for complex conjugate [35]. This singular expansion can be dealt with using $\lim_{\eta \rightarrow 0^+} [1/(x - x_0 - i\eta)] = \text{P}[1/(x - x_0)] + i\pi \delta(x - x_0)$ where P stands for principal value, and the CDOS defined by Eq. (1) can be rewritten as

$$\rho(\mathbf{r}, \mathbf{r}', \omega) = \sum_n \text{Tr} [\mathbf{e}_n(\mathbf{r}, \omega) \mathbf{e}_n^*(\mathbf{r}', \omega)] \delta(\omega - \omega_n) . \quad (2)$$

*Electronic address: remi.carminati@espci.fr

This expression explicitly shows that the CDOS sums up all eigenmodes connecting \mathbf{r} to \mathbf{r}' at frequency ω , weighted by their strength at both points \mathbf{r} and \mathbf{r}' . In the case of an open and/or absorbing system, a frequent situation in nanophotonics or plasmonics, the rigorous introduction of a basis of eigenmodes is more involved (an approach has been proposed recently in the quasi-static approximation [36]). Assuming weak leakage, quasi-modes can be introduced in a phenomenological way, by broadening the eigenmodes using a linewidth γ_n . This results in an expansion similar to (2) with a Lorentzian lineshape replacing the delta function. The eigenmode expansion of the CDOS gives a rigorous basis to the network picture put forward above. It is important to note that, using Eq. (1), the correct counting of modes is automatically performed in the calculation of the imaginary part of the dyadic Green function, even when a basis of eigenmodes cannot be explicitly calculated or even rigorously defined.

We shall now show that the concept of CDOS allows us to clarify an important issue in nanophotonics concerning light scattering and localization in disordered fractal metallic films. These peculiar structures exhibit optical properties that strongly differ from those of bulk metals or ensembles of isolated nanoparticles [27]. The interplay between surface-plasmon resonances and multiple scattering by the fractal percolation clusters leads to spatial concentration of light in subwavelength areas (hot spots) [37, 38]. The theoretical description of this phenomenon has been the subject of a controversy. Using a scaling theory in the quasi-static approximation, a mechanism based on Anderson localization has been put forward [39]. This approach has been questioned by numerical simulations showing that at a given frequency, localized and delocalized plasmonic eigenmodes were expected to coexist, a situation referred to as inhomogeneous localization [28] (localized eigenmodes have a spatial extent smaller than the sample size, while delocalized eigenmodes spread over the whole sample). Measurements of intensity fluctuations in the near field have led to the conclusion that both kind of eigenmodes should coexist [29], in agreement with expectations resulting from numerical simulations [30], and that localized modes should dominate around the percolation threshold (but not exactly at percolation). More recently, measurements of near-field LDOS statistics have confirmed the existence of spatially localized modes in the regime dominated by fractal clusters (close to the percolation threshold) [8]. We shall now demonstrate that the use of the CDOS unambiguously describes this spatial squeezing of eigenmodes, providing a solid theoretical basis to the most recent observations. We introduce the intrinsic coherence length as a natural measure of the overall spatial extent sustained by the full set of eigenmodes. This clarifies a fundamental issue in the optics of disordered fractal films.

The CDOS can be calculated numerically using exact three-dimensional simulations. We summarize the procedure that is fully described in Ref. [40]. Semi-continuous gold films are generated using a Kinetic Monte-Carlo

algorithm, reproducing the geometrical features or real films. Typical realizations of films are shown in the top row in Fig. 1 (with gold in black color). To calculate the electric dyadic Green function $\mathbf{G}(\mathbf{r}, \mathbf{r}', \omega)$, we need to calculate the electric field at a position \mathbf{r} generated by a point electric-dipole source \mathbf{p} located at position \mathbf{r}' . To proceed, we solve numerically the Lippmann-Schwinger equation:

$$\mathbf{E}(\mathbf{r}) = \mathbf{E}_0(\mathbf{r}) + \frac{\omega^2}{c^2} [\epsilon(\omega) - 1] \int_V \mathbf{G}_0(\mathbf{r}, \mathbf{r}_1, \omega) \mathbf{E}(\mathbf{r}_1) d^3 r_1 \quad (3)$$

where \mathbf{G}_0 is the vacuum dyadic Green function, $\mathbf{E}_0(\mathbf{r}) = \mu_0 \omega^2 \mathbf{G}_0(\mathbf{r}, \mathbf{r}', \omega) \mathbf{p}$ the incident field, $\epsilon(\omega)$ the dielectric function of gold and V the volume occupied by the gold film. The full dyadic Green function is deduced from $\mathbf{E}(\mathbf{r}) = \mu_0 \omega^2 \mathbf{G}(\mathbf{r}, \mathbf{r}', \omega) \mathbf{p}$. The computation of the LDOS and CDOS follows from Eq. (1).

We show in Fig. 1 the LDOS maps (middle row) and CDOS maps (bottom row) computed in a plane at a distance $z = 40$ nm above two different films (shown in the top row) corresponding to two different regimes. For $f = 20\%$ (left column), the film is composed of isolated nanoparticles whereas for $f = 50\%$ (right column) the film is close to the percolation threshold, a regime in which fractal clusters dominate (multiscale resonant regime) [8, 27, 40]. Before studying spatial coherence and the extent of eigenmodes based on the CDOS, let us summarize here the main features of the LDOS maps [23, 40]. For low surface fraction (left column), LDOS peaks are observed on top of isolated nanoparticles that are resonant at the observation wavelength. A correspondence between LDOS peaks and the position of one or several nanoparticles is easily made. For a different observation wavelength (not shown for brevity), particles can switch on or off resonance and the position of the LDOS peaks changes, but remain attached to individual particles. The sample behaves as a collection of individual nanoparticles with well identified surface plasmon resonances. In the multiscale resonant regime (right column), the LDOS structure is more complex. The connection between the film topography and the localized field enhancements (that are responsible for LDOS spatial fluctuations) cannot be established on a simple one-to-one correspondence, a known feature of fractal metallic films [28, 37, 38].

The maps of the CDOS $\rho(\mathbf{r}, \mathbf{r}', \omega)$ (bottom row in Fig. 1) are displayed versus \mathbf{r} for a fixed position \mathbf{r}' (chosen at the center of the sample). Their meaning can be understood as follows: They display the ability of a point \mathbf{r} at a given distance from the center point \mathbf{r}' to be connected to this center point by the underlying structure of the optical eigenmodes. For example, a large CDOS (larger than the vacuum CDOS) would allow two quantum emitters at \mathbf{r} and \mathbf{r}' to couple efficiently. It would also ensure coherent (correlated) fluctuations of the light fields at \mathbf{r} and \mathbf{r}' under thermal excitation [31]. The CDOS also allows one to discriminate between two hot spots at \mathbf{r} and \mathbf{r}' that belong to the same eigenmode (or

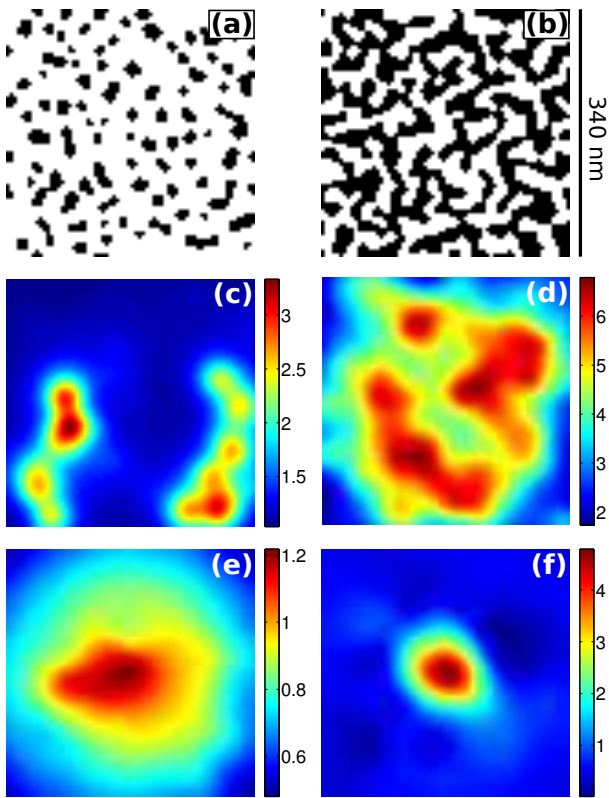


FIG. 1: (Color online) (a),(b): Geometry of the disordered films generated numerically (with gold in black color). (a): $f = 20\%$, (b): $f = 50\%$. (c),(d): Maps of the normalized LDOS $\rho(\mathbf{r}, \omega)/\rho_0(\omega)$ calculated in a plane at a distance $z = 40$ nm above the film surface, $\rho_0(\omega)$ being the LDOS in vacuum. (e),(f): Maps of the normalized CDOS $\rho(\mathbf{r}, \mathbf{r}', \omega)/\rho_0(\omega)$ with \mathbf{r}' fixed at the center of the sample. $\lambda = 780$ nm.

that are connected by at least one eigenmode), or that are completely independent. Last but not least, since the CDOS implicitly sums up the spatial extent of the full set of eigenmodes, it appears as a natural tool to describe the overall spatial localization in the multiscale resonant regime. It is striking to see that the extent of the CDOS in the multiscale resonant regime (Fig. 1f) is reduced to a smaller range compared to the case of a film composed of isolated nanoparticles (Fig. 1e). This means that although long-range (delocalized) eigenmodes do exist in the multiscale resonant regime, the weight of localized eigenmodes (with a spatial extent smaller than the sample size) is larger (remember that the CDOS is implicitly a weighted sum over the full set of eigenmodes). The reduction of the extent of the CDOS clearly demonstrates an overall spatial squeezing of the eigenmodes close to the percolation threshold, in agreement with the accepted picture. Let us stress that the approach based on the CDOS gives a non-ambiguous description of this overall spatial squeezing, without assuming the existence of an Anderson localization length [28, 29]. It is based on a concept implicitly related to field-field spatial correlations as in classical spatial coherence theory, that seems

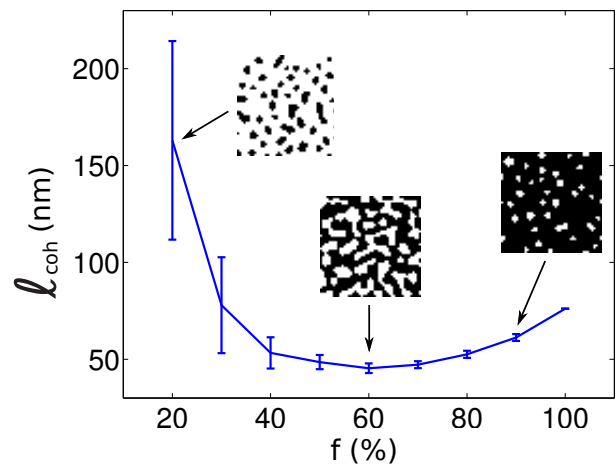


FIG. 2: (Color online) Averaged value (solid line) and variance (error bars) of the intrinsic coherence length ℓ_{coh} calculated at a distance $z = 40$ nm above a disordered film, versus the gold surface fraction f . $\lambda = 780$ nm. Inset: Typical film geometries (black color corresponds to gold).

to carry sufficient information to describe one of the most striking features in the optics of disordered fractal metallic films.

In order to quantify the overall reduction of the spatial extent of eigenmodes in the multiscale resonant regime, we can introduce an intrinsic coherence length ℓ_{coh} , defined from the width of the CDOS. More precisely, fixing \mathbf{r}' at the center of the sample, we use polar coordinates in the plane $z = 40$ nm parallel to the sample mean surface to write $\rho(\mathbf{r}, \mathbf{r}', \omega) = \rho(R, \theta, \omega)$ with $R = |\mathbf{r} - \mathbf{r}'|$ and define an angularly-averaged CDOS $\bar{\rho}(R, \omega) = (2\pi)^{-1} \int_0^{2\pi} \rho(R, \theta, \omega) d\theta$. The intrinsic coherence length ℓ_{coh} is defined as the width of $\bar{\rho}(R, \omega)$ considered as a function of R . It is important to note that ℓ_{coh} is not necessarily the size of the hot spots observed on the surface, since a given eigenmode can be composed of several hot spots. Two different hot spots separated by a distance smaller than ℓ_{coh} can be intrinsically connected (meaning that they are connected by at least one eigenmode). As mentioned above, the ability to clarify this distinction between eigenmodes and hot spots is an essential feature of the CDOS. The averaged value of $\langle \ell_{\text{coh}} \rangle$ (solid line) and its variance $\text{Var}(\ell_{\text{coh}})$ (error bars) are shown in Fig. 2 versus the film surface fraction. Both quantities are calculated using a statistical ensemble of realizations of disordered films generated numerically (the error bars indicate the real variance of ℓ_{coh} , and not computations errors due to lack of numerical convergence, the latter being ensured by a sufficiently large set of realizations). We observe a minimum of $\langle \ell_{\text{coh}} \rangle$ for a surface fraction close to the percolation threshold. This unambiguously demonstrates the overall spatial squeezing of eigenmodes in the regime dominated by fractal clusters. Our approach provides a solid theoretical description of this phenomenon, that has been indirectly observed experimentally from measurements of LDOS

fluctuations [8]. Note that in this experimental study, the inverse participation ratio was used to connect qualitatively the spatial extent of eigenmodes to the variance of the LDOS fluctuations, permitting only a qualitative comparison with the curve in Fig. 2 (the inverse participation ratio and the intrinsic coherence length cannot be compared directly). The precise shape of the curve might also be influenced by finite-size effects inherent to the numerical calculations (the calculations probably overestimates the weight of extended eigenmodes). The behavior of $\text{Var}(\ell_{\text{coh}})$ is also instructive. Strong fluctuations are observed in the regime of isolated nanoparticles, a signature of the strong fluctuations of the distance between individual particles that directly influences ℓ_{coh} . Conversely, in the multiscale resonant regime, the reduction of the fluctuations reinforces the assumption of a

mechanism based on collective interactions that involve the sample as a whole.

In summary, we have shown that the CDOS characterizes the intrinsic spatial coherence of a photonic or plasmonic system, independently on the illumination conditions. Using this concept, we have demonstrated unambiguously the spatial squeezing of plasmonic eigenmodes on disordered fractal metallic films close to the percolation threshold. This clarifies a basic issue in plasmonics concerning the description of the optical properties of these films. This illustrates the relevance of the CDOS in the study of spatial coherence in photonics and plasmonics systems, and more generally in wave physics.

We acknowledge Y. De Wilde, M. Kociak, V. Krachmalnicoff and R. Sapienza for stimulating discussions.

-
- [1] U. Kreibig and M. Vollmer, *Optical Properties of Metal Clusters* (Springer, Berlin, 1995).
- [2] L. Novotny and B. Hecht, *Principles of Nano-Optics* (Cambridge University Press, Cambridge, 2006).
- [3] M.I. Stockman, *Opt. Express* **19**, 22029 (2011).
- [4] J.D. Joannopoulos, R.D. Meade and J. N. Winn, *Photonic Crystals: Molding the Flow of Light*, 2nd edition (Princeton University Press, Princeton, 2008).
- [5] D. R. Smith, J. B. Pendry, M. C. K. Wiltshire, *Science* **305**, 788 (2004).
- [6] P. Sheng, *Introduction to Wave Scattering, Localization, and Mesoscopic Phenomena* (Academic Press, San Diego, 1995).
- [7] M. Durach, A. Rusina, and M.I. Stockman, *Nano Lett.* **7**, 3145 (2007).
- [8] V. Krachmalnicoff, E. Castanié, Y. De Wilde and R. Carminati, *Phys. Rev. Lett.* **105**, 183901 (2010).
- [9] L. Sapienza *et al.*, *Science* **327**, 1352 (2010).
- [10] R. Sapienza, *et al.*, *Phys. Rev. Lett.* **106**, 163902 (2011).
- [11] D.E. Chang, A.S. Sorensen, E.A. Demler and M.D. Lukin, *Nature Phys.* **3**, 807 (2007).
- [12] S. Aberra Guebrou *et al.*, *Phys. Rev. Lett.* **108**, 066401 (2012).
- [13] P. A. Huidobro, A. Y. Nikitin, C. González-Ballester, L. Martín-Moreno and F.J. García-Vidal, arXiv:1201.6492v1.
- [14] J. Seelig *et al.*, *Nano Lett.* **7**, 685 (2007).
- [15] X. Li and M.I. Stockman, *Phys. Rev. B* **77**, 195109 (2008).
- [16] A. Sentenac and P.C. Chaumet, *Phys. Rev. Lett.* **101**, 013901 (2008).
- [17] I. M. Vellekoop, A. Lagendijk, and A. P. Mosk, *Nature Photon.* **4**, 320 (2010).
- [18] J. Verbeeck, D. van Dyck, H. Lichte, P. Potapova and P. Schattschneider, *Ultramicroscopy* **102**, 239 (2005).
- [19] Y. De Wilde *et al.*, *Nature* **444**, 740 (2006).
- [20] A. Trügler, J.-C. Tinguely, J.R. Krenn, A. Hohenau and U. Hohenester, *Phys. Rev. B* **83**, 081412(R) (2011).
- [21] S. Mazucco *et al.*, *Nano Lett.* **12**, 1288 (2012).
- [22] R. Vincent and R. Carminati, *Phys. Rev. B* **83**, 165426 (2011).
- [23] E. Castanié, V. Krachmalnicoff, A. Cazé, R. Pierrat, Y. De Wilde and R. Carminati, *Opt. Lett.*, in press (2012).
- [24] J. de Rosny and M. Fink, *Phys. Rev. Lett.* **89**, 124301 (2002).
- [25] R. Carminati, R. Pierrat, J. de Rosny and M. Fink, *Opt. Lett.* **32**, 3107 (2007).
- [26] G. Lerosey, J. de Rosny, A. Tourin and M. Fink, *Science* **315**, 1120-1122 (2007).
- [27] V. M. Shalaev, *Nonlinear Optics of Random Media* (Springer, Berlin, 2000).
- [28] M.I. Stockman, S.V. Faleev and D.J. Bergman, *Phys. Rev. Lett.* **87**, 167401 (2001).
- [29] K. Seal *et al.*, *Phys. Rev. Lett.* **97**, 206103 (2006).
- [30] D.A. Genov, A.K. Sarychev and V.M. Shalaev, *Phys. Rev. E* **67**, 056611 (2003).
- [31] K. Joulain, J.P. Mulet, F. Marquier, R. Carminati and J.-J. Greffet, *Surf. Sci. Rep.* **57**, 59 (2005).
- [32] R.L. Weaver and O.I. Lobkis *Phys. Rev. Lett.* **87**, 134301 (2001); E. Larose *et al.*, *Geophysics* **71**, S11 (2006).
- [33] T. Setälä, K. Blomstedt, M. Kaivola and A.T. Friberg, *Phys. Rev. E* **67**, 026613 (2003).
- [34] The LDOS $\rho(\mathbf{r}, \omega) = 2\omega/(\pi c^2) \text{Im} [\text{Tr} \mathbf{G}(\mathbf{r}, \mathbf{r}, \omega)]$ enters the expression of the spontaneous decay rate of an atom with an electric dipole transition [2], and of the electric energy density in a system at thermal equilibrium. For magnetic dipole transitions, or for the computation of the full equilibrium energy density, an additional magnetic term has to be added, see K. Joulain, R. Carminati, J.P. Mulet and J.-J. Greffet, *Phys. Rev. B* **68**, 245405 (2003).
- [35] P.M. Morse and H. Feshbach, *Methods of Theoretical Physics* (McGraw-Hill, New York, 1953), chap. 13.
- [36] G. Boudarham and M. Kociak, *Phys. Rev. B* **85**, 245447 (2012).
- [37] S. Grésillon *et al.*, *Phys. Rev. Lett.* **82**, 4520 (1999).
- [38] J. Laverdant, S. Buil, B. Bérini and X. Quélin, *Phys. Rev. B* **77**, 165406 (2008).
- [39] A.K. Sarychev, V.A. Shubin and V.M. Shalaev, *Phys. Rev. B* **60**, 16389 (1999).
- [40] A. Cazé, R. Pierrat and R. Carminati, *Photon Nanostruct: Fundam Appl*, in press (2012), <http://dx.doi.org/10.1016/j.photonics.2012.03.001>